Synthesis, Binding Properties, and ^{18}F Labeling of Fluorocarazolol, a High-Affinity β-Adrenergic Receptor Antagonist

Lei Zheng,* Marc S. Berridge, and Paul Ernsberger

Departments of Radiology and Chemistry, Case Western Reserve University School of Medicine and University Hospitals of Cleveland, Cleveland, Ohio 44106

Received April 1, 1994®

New β-adrenergic receptor antagonists, 2-(*R*)-(+)- and 2-(S)-(−)-1-(9*H*-carbazol-4-yl-oxy)-3-[[1-(fluoromethyl)ethyl]amino]-2-propanol ((*S*)- and (*R*)-fluorocarazolols), were labeled with fluorine-18 at the no-carrier-added level by reductive alkylation of desisopropylcarazolol (4-(2-hydroxy-3-amino-1-propoxy)carbazole) with [^{18}F]fluoroacetone. The latter was prepared by nucleophilic substitution of fluoride on acetol tosylate and may serve as a useful synthetic precursor for other radiotracers. The radiochemical yield of [^{18}F]fluorocarazolol (500−1200 Ci/mmol) from [^{18}F]fluoride was 40 ± 10% at the end of the 45 min synthesis. Chiral HPLC showed >99% enantiomeric purity of 2-(*S*)- and 2-(*R*)-[^{18}F]fluorocarazolols. The log *P* of fluorocarazolol was 2.2 at pH 7.4. The *in vitro* K_D values of (*S*)- and (*R*)-fluorocarazolol for the β-adrenergic receptor were measured in a rat heart preparation to be K_D = 68 and 1128 pM, respectively. Biodistribution experiments in mice demonstrated specific β-adrenergic receptor binding of (*S*)-[^{18}F]fluorocarazolol. (*R*)-[^{18}F]fluorocarazolol showed no observable specific binding to β-receptors *in vivo*. The uptake of (*R*)-[^{18}F]fluorocarazolol may therefore be used as an estimation of nonspecific binding. Positron emission tomography images of pigs showed receptor-specific uptake of (*S*)-[^{18}F]fluorocarazolol in the heart and lung. Washout of dissociated ligand from the tissue was observed only after 70 min postinjection. The maximum ratio of specific to nonspecific uptake in pig heart and lung was ca. 10 at 150 min postinjection. Observed levels of fluorocarazolol metabolites in mouse and pig blood were relatively low and remained fairly constant during the period from 10 to 180 min postinjection. These results indicate that (*S*)-(−)-[^{18}F]fluorocarazolol is of interest for use as a radiopharmaceutical for estimation of β-adrenergic receptors with positron tomography.

Introduction

β-Adrenergic receptors play a role in many diseases of the heart and the brain. They have been shown to be altered in the brains of patients suffering from schizophrenia, Alzheimer's disease, panic disorder, aging, fear, anxiety, depression, and stress[1−7]. They may also play a role in the regulation[2,7,8] of normal behavior. In heart disease, β-receptors are altered in heart failure and in ischemia and infarction, important classes of heart disease.[9] In both organs, the receptor concentrations are also altered[7,10,11] by the action of hormones and drugs used in treatment. Changes in receptor concentration, whether due to disease or treatment, produce a variation in tissue response to catecholamines. We are therefore interested in assessing receptor concentration *in vivo* by positron emission tomography (PET) for the investigation of disease etiology and progression and possibly in diagnosis and treatment. Iodopindolol and iodocyanopindolol[12−16] have been labeled with radioiodine and used for *in vitro* determination of β-receptor densities. Though radioiodine can be used in single-photon tomography (SPECT) imaging,[17] the properties of the iodine label makes these compounds unsuitable for PET measurement of β-receptors. PET with labeled high-affinity receptor ligands and an appropriate kinetic model[18−23] allows noninvasive *in vivo* assessment of regional receptor concentrations. Several β-adrenergic ligands have been labeled in attempts to measure β-adrenergic receptors *in vivo* using PET. Propranolol,[24] practolol,[25] and pindolol[26] were labeled with ^{11}C for PET use, but specific binding to receptors *in vivo* was not observable. Though these drugs are clinically effective, their affinity for the receptor was insufficient to produce the lasting, high proportion of specific binding necessary for *in vivo* visualization. In contrast to other well-known (dopamine and serotonin) receptors, specific binding to β-adrenergic receptors seems to become observable by PET only as the *in vitro* ligand−receptor dissociation constant of a labeled antagonist drops below 300 pM. High-affinity ligands, [^{11}C]-(*S*)-carazolol[27] and [^{11}C]CGP 12177,[28,29] are the only ligands available that can be used to observe specific binding of β-adrenergic receptors. Unfortunately, both of these ligands present experimental difficulties. The decay rate of the ^{11}C label of carazolol is too fast to allow accurate measurement of its slow rate of receptor−ligand complex dissociation (k_4). Because this rate is an important parameter in the mathematical model[18−23] used to analyze binding data, inaccuracy in its measurement can reduce the accuracy of a receptor estimation. CGP 12177 has also been labeled with ^{11}C; however a standard kinetic model could not be used[28] for analysis. Known structure−activity relationships for β-adrenergic antagonists suggested that 1″-fluorocarazolol, an analog of carazolol, should have a receptor affinity similar to that of carazolol itself, although the substitution of fluorine could alter[30] the affinity ratio of β_1- to β_2-receptor subtypes. The use of ^{18}F as a label, with its half-life of 109.8 min as compared to the 20 min half-life of ^{11}C,

* Corresponding author (forwarding address): Division of Radiation Sciences, Washington University School of Medicine, 510 S. Kingshighway Blvd., St. Louis, MO 63110. Telephone: (314) 362-8428. Fax: (314) 362-8399. email: zheng@petchem1.wustl.edu.

® Abstract published in *Advance ACS Abstracts*, August 15, 1994.

0022-2623/94/1837-3219$04.50/0

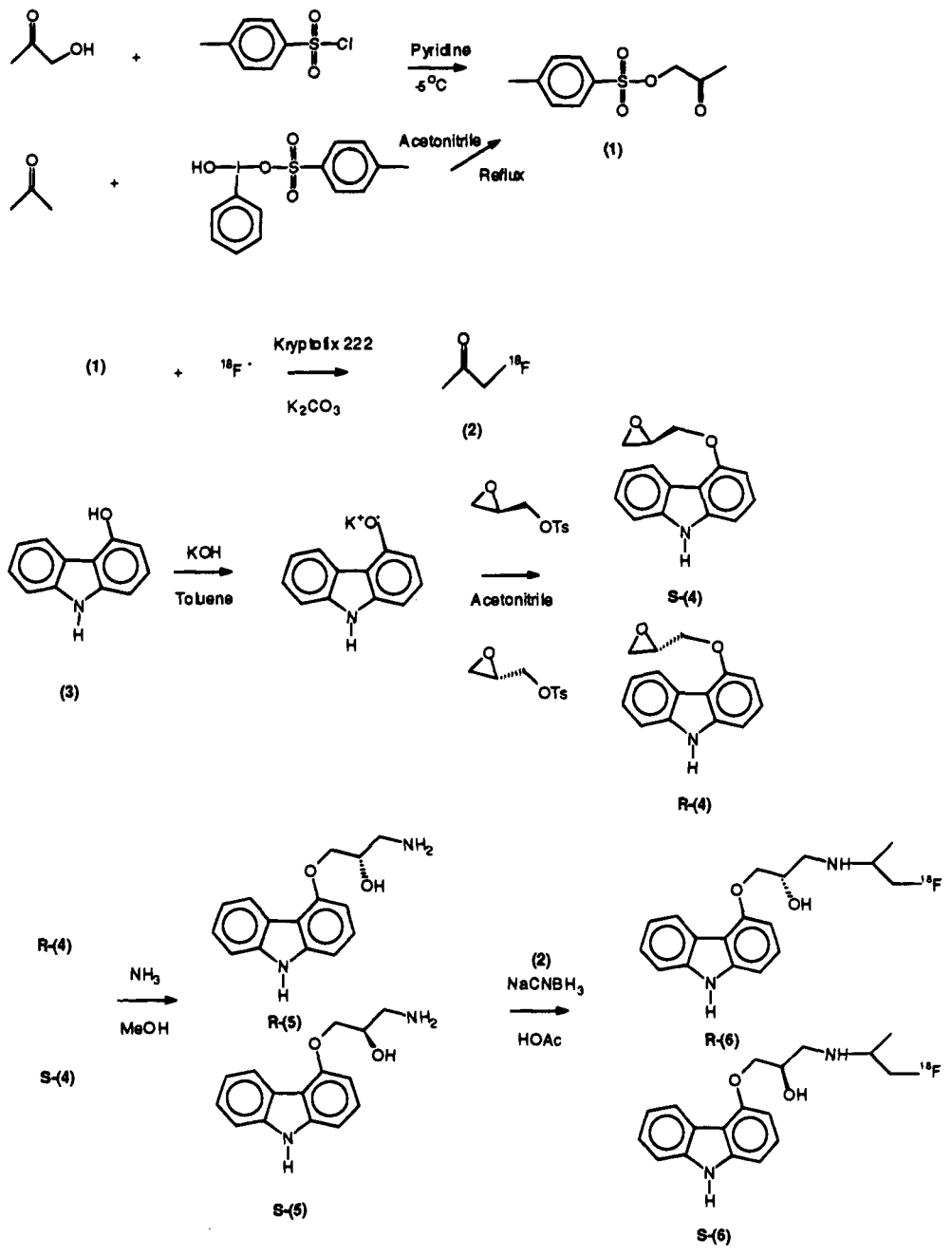

Figure 1. Synthesis of (*R*)- and (*S*)-[^{18}F]fluorocarazolol.

will allow collection of data for a sufficient time to estimate a rate constant (k_4) with an expected half-time of 1–3 h. We therefore chose to label fluorocarazolol with fluorine-18 and test its properties for the PET study of β-adrenergic receptors *in vivo*.

Chemistry

The synthesis of [^{18}F]fluorocarazolol is shown in Figure 1. Acetol tosylate (**1**) was used as a substrate for nucleophilic substitution with [^{18}F]fluoride. It was synthesized by two different methods according to the amount of product required. To produce large quantities of **1**, the reaction of acetol with tosyl chloride was used. Though the yield was relatively low (10–15%), the materials were inexpensive and readily available. For small quantities, α-tosylation of acetone with hydroxy(tosyloxy)iodobenzene was more convenient and gave a higher yield (55–60%). Reaction of acetol tosylate with [^{18}F]fluoride under standard conditions yielded [^{18}F]fluoroacetone (**2**) in 60 ± 7% yield.

Desisopropylcarazolol (**5**) was prepared with specific chirality according to Berridge et al.[27] in five steps. It was recently reported[31] that another group used this procedure for conversion of 4-hydroxycarbazole (**3**) to 4-(2,3-epoxypropoxy)carbazole (**4**) with enantiomerically pure glycidyl tosylate and observed greater than 10% racemization. It was proposed[32] that the sulfonate leaving group be changed to reduce the degree of racemization. However, in our hands, chiral HPLC analysis has shown that both the *R* and *S* enantiomers of **5** were produced with greater than 99% enantiomeric purity by the originally published[27] route. The analysis was performed indirectly by using the final products of interest. *R*, *S*, and racemic samples of **5** were prepared from commercial glycidyl tosylate of corresponding chirality. Fluorocarazolol and carazolol (produced by the analogous reaction using acetone[27] in place of fluoroacetone) were then prepared from the different samples of **5** and analyzed (Figure 2). No detectable

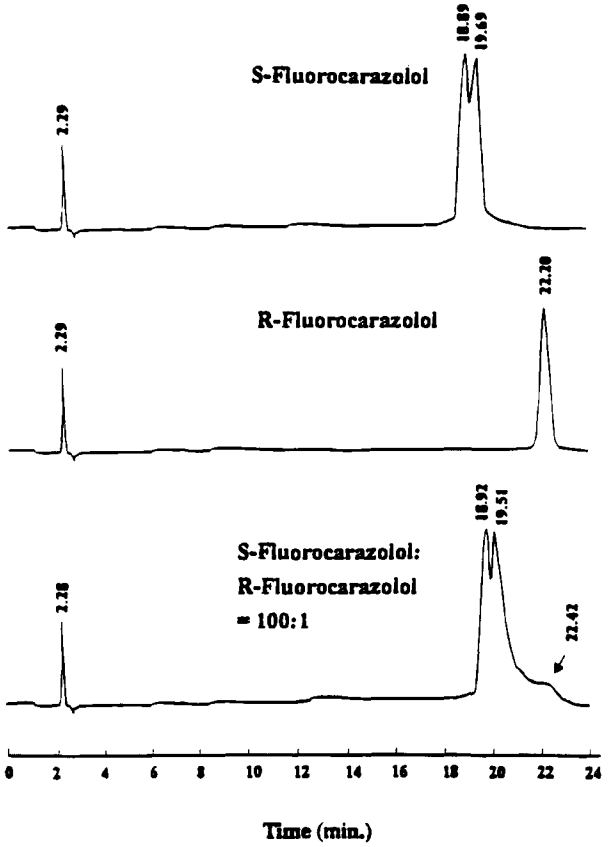

Figure 2. Chiral HPLC analysis of (*R*)- and (*S*)- fluorocarazolol. On a Nacherey-Nagel nucleosil chiral 2 column eluted with 54% THF, in *n*-heptane (with 0.5%, v/v, trifluoroacetic acid), the two diastereomers of (*S*)-fluorocarazolol were further separated (top chromatogram) while the two diastereomers of (*R*)-fluorocarazolol were resolved (middle chromatogram). Coinjection of 1% (*R*)-fluorocarazolol in (*S*)-fluorocarazolol gave three measurable peaks (bottom chromatogram). Numbers listed on the top of the peaks are retention times.

racemization was present in either the carazolol or fluorocarazolol samples prepared from either enantiomer of **5**. The limit of detection was well below 1% (Figure 2). It is likely that our use of the azeotropically dried 4-hydroxycarbazole salt for the synthesis of **4** was necessary to avoid racemization, though we have not performed the synthesis without the drying step. An additional feature is observable in Figure 2. There are four possible diastereomers of fluorocarazolol because the asymmetry of fluoroacetone causes a second chiral center to be introduced during the reductive alkylation. The two diastereomers derived from (*S*)-desisopropylcarazolol (2-(*S*)-fluorocarazolols) were separated on a chiral analytical column with retention times of 18.9 and 19.7 min. The two diastereomers derived from (*R*)-desisopropylcarazolol (2-(*R*)-fluorocarazolols) were not separated under the same conditions and gave a single peak at 22.2 min. The purpose of the chirality analysis was only to verify stereoisomeric purity at the 2 position. Though diastereomers of 2-(*S*)-fluorocarazolol were observed, they were not separated for any further experiments.

Purified [^{18}F]fluoroacetone (**2**) was reacted with **5** using sodium cyanoborohydride as the reducing agent to give [^{18}F]fluorocarazolol (**6**). From a typical [^{18}F]-fluoride production run (15 μA bombardment for 45 min, yielding 620 mCi of $^{18}F^-$), 50 mCi of $^{18}F^-$ was removed for [^{18}F]fluorocarazolol synthesis. At 45 min after the [^{18}F]fluoride was introduced, 16 mCi of HPLC-purified [^{18}F]fluorocarazolol was obtained with a specific activity of 500–1200 Ci/mmol.

Table 1. Measured log *P* Values of [^{18}F]Fluorocarazolol and [^{11}C]Carazolol at Different pH Values

	log *P*			log *P*	
pH	fluorocarazolol	carazolol	pH	fluorocarazolol	carazolol
3.3	0.03	0.17	7.5	2.48	1.51
4.5	0.38	0.30	8.3	2.70	2.13
5.8	1.11	0.42	9.4	2.80	2.44
6.4	1.76	0.68	10.0	2.81	2.50
7.0	2.20	1.07	10.8	2.81	2.43

In order to characterize **6**, nonradioactive (*R*)- and (*S*)-fluorocarazolols were prepared by essentially the same method shown in Figure 1 using commercially available fluoroacetone. In this reaction, an excess of sodium cyanoborohydride was observed to cause the production of another compound which was not fully identified but whose mass spectrum indicated the presence of boron. This compound coeluted with fluorocarazolol on the preparative HPLC system, and no other chromatographic system was found which could separate them. To prevent the formation of the boron-containing compound, sodium cyanoborohydride was purified by crystallization before use and was used at slightly less than a stoichiometric ratio (mole ratio etic acid in the reaction solution). The fluorocarazolol which was obtained was a white solid which decomposed within a few weeks when exposed to air at room temperature. The product was successfully stabilized by preparation of the hydrochloride salt.

Biological Results

Octanol–Water Partition Coefficient. The lipophilicity of a radiotracer affects its tissue permeability properties, and thus its ability to enter target tissues. The octanol–water partition coefficients (*P*) at different pH values of [^{18}F]fluorocarazolol and, for comparison, [^{11}C]carazolol[15] were therefore measured. The results are shown in Table 1. Since the amino function depends on the pH of the media, the partition coefficient of fluorocarazolol can be considered as a function of the partition coefficients of the free base, *P*(B), and the protonated amine, P(BH):

$$P = \frac{P(B)}{1 + 10^{[pK_a - pH]}} + \frac{P(BH)}{1 + 10^{[pH - pK_a]}} \qquad (1)$$

From the measured partition coefficients as a function of pH, the fluorocarazolol parameters in eq 1 were determined by a least-squares curve fit to be $P(B) = 645$, $P(BH) = 1.0$, and $pK_a = 7.5$. The parameters similarly calculated for carazolol were $P(B) = 302$, $P(BH) = 1.7$, and $pK_a = 8.4$.

***In Vitro* Binding.** The measured binding affinities (K_d, pM) of (*R*)- and *S*-fluorocarazolol to β-adrenergic receptors in rat heart tissue were 1128 ± 113 and 68 ± 8, respectively. The values obtained for comparison with (*R*)- and (*S*)-carazolol were 404 ± 50 and 22 ± 3. The experimental data are shown in Figure 3. A competitive binding assay against iodopindolol was used. The values obtained for (*R*)- and (*S*)-carazolol agree with reported[33,34] literature values. Though the

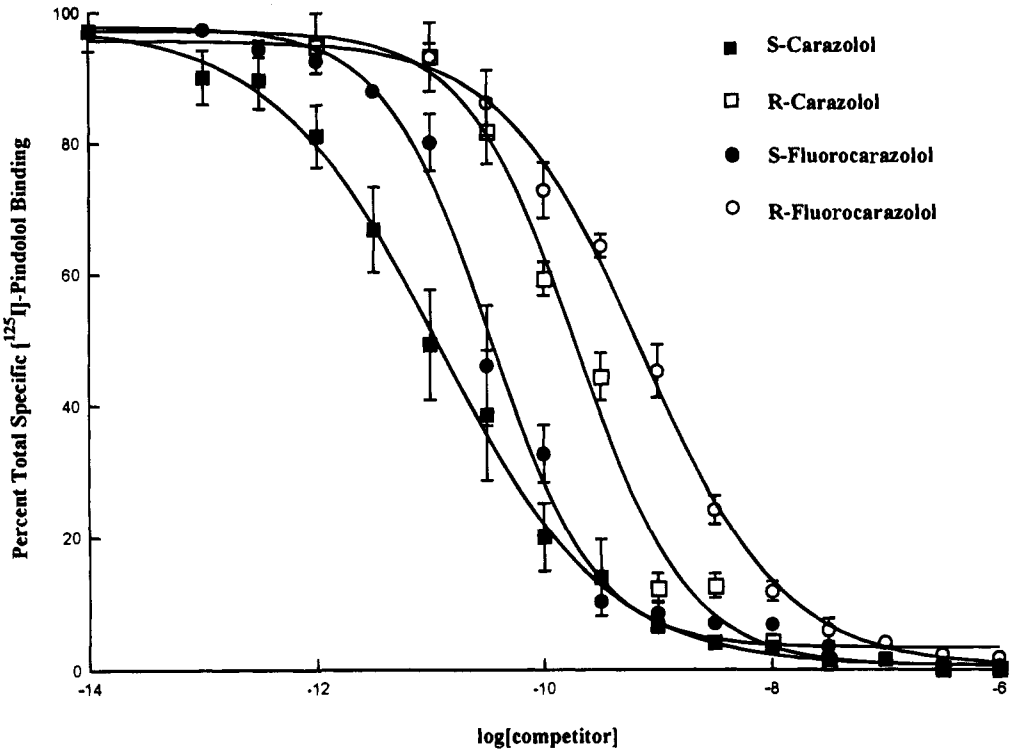

Figure 3. Inhibition of [^{125}I]iodopindolol binding to rat heart membranes by increasing concentrations of carazolol analogs. Data are the percentages of total specific binding as defined by 0.1 mM (−)-isoproterenol, mean ± standard deviation for four experiments, each conducted in triplicate. Curves were generated by nonlinear fit to the logistic equation using InPlot (GraphPAD software, San Diego, CA). Binding affinities derived from the curve were (expressed as K_d): (*S*)-fluorocarazolol, 68 ± 8 pM; (*R*)-fluorocarazolol, 1128 ± 113 pM; (*S*)-carazolol, 22 ± 3 pM and (*R*)-carazolol, 404 ± 50 pM.

Table 2. Tissue Distribution of (*S*)-[^{18}F]Fluorocarazolol in Mouse Organs[a]

	time (min)	blood	heart	lung	brain	liver	kidney	bone
nonpro*	10	0.56 ± 0.07	1.10 ± 0.17	6.40 ± 0.58	1.18 ± 0.18	3.55 ± 0.27	4.18 ± 0.54	0.65 ± 0.03
nonpro	20	0.71 ± 0.16	0.91 ± 0.13	7.46 ± 1.96	0.95 ± 0.13	2.54 ± 0.05	2.89 ± 0.67	0.65 ± 0.12
nonpro	40	0.69 ± 0.16	0.77 ± 0.14	6.16 ± 3.06	1.09 ± 0.36	1.70 ± 0.55	2.01 ± 0.44	0.71 ± 0.19
nonpro	60	0.60 ± 0.10	0.61 ± 0.07	5.34 ± 1.20	0.81 ± 0.03	1.32 ± 0.50	1.39 ± 0.39	0.72 ± 0.18
nonpro	90	0.66 ± 0.15	0.61 ± 0.12	5.88 ± 1.06	0.80 ± 0.16	1.09 ± 0.22	1.33 ± 0.39	1.13 ± 0.17
nonpro	120	0.52 ± 0.18	0.45 ± 0.14	4.82 ± 1.78	0.64 ± 0.22	0.96 ± 0.10	0.83 ± 0.35	1.08 ± 0.22
nonpro	180	0.43 ± 0.04	0.40 ± 0.06	4.80 ± 0.36	0.67 ± 0.10	0.88 ± 0.15	0.71 ± 0.11	1.90 ± 0.42
pro**	10	0.39 ± 0.10	1.06 ± 0.39	5.00 ± 1.98	1.23 ± 0.32	2.89 ± 0.38	4.18 ± 0.35	0.72 ± 0.21
pro	20	0.43 ± 0.10	0.63 ± 0.10	3.26 ± 0.72	0.78 ± 0.27	1.85 ± 0.32	2.19 ± 0.43	0.86 ± 0.52
pro	40	0.35 ± 0.07	0.51 ± 0.14	1.98 ± 0.30	0.64 ± 0.22	1.66 ± 0.29	1.64 ± 0.38	0.64 ± 0.14
pro	60	0.25 ± 0.10	0.29 ± 0.12	1.10 ± 0.30	0.25 ± 0.15	1.17 ± 0.68	1.28 ± 0.72	1.10 ± 0.45
pro	90	0.34 ± 0.08	0.35 ± 0.05	1.06 ± 0.22	0.38 ± 0.11	1.39 ± 0.31	0.92 ± 0.11	0.72 ± 0.17
pro	120	0.13 ± 0.04	0.15 ± 0.04	0.52 ± 0.24	0.11 ± 0.04	0.66 ± 0.21	0.38 ± 0.18	1.42 ± 0.66
pro	180	0.15 ± 0.08	0.15 ± 0.09	0.72 ± 0.20	0.09 ± 0.05	0.59 ± 0.29	0.35 ± 0.19	2.72 ± 0.57

[a] Uptake is expressed as (unitless) fractional dose per fractional body weight of the organ. Values are expressed as average ± SD. Data points for heart, brain, blood, lung, kidney, liver, and bone represent five mice at each data point. Data points for other organs represent at least three mice. *: no propranolol preadministration. **: with propranolol preadministration.

affinity of (*S*)-fluorocarazolol for the receptor is less than that of (*S*)-carazolol, with a K_d under 100 pM, it can still be described as a very high affinity ligand. Inhibition binding in this tissue by (−)-isoproterenol gave the biphasic curve expected from an agonist.[35] Fluorocarazolol (Figure 3) gave a monophasic curve indicative of an antagonist.[35] Moreover, the fluorocarazolol curve was similar in shape to and only slightly shifted by a lower receptor affinity than that of the parent compound carazolol, a known receptor antagonist. To further verify the antagonism of (*S*)-fluorocarazolol, heart rate observations were performed in mice. Propranolol (88 mg/kg) altered heart rate from a base line average of 690 to 300 min^{-1} ($p \ll 0.001$); fluorocarazolol and carazolol (5.5 mg/kg) lowered heart rate from a base line of 640 to 370^{-1} ($p \ll 0.001$) and 420 min^{-1} ($p < 0.001$), respectively. Control mice had heart rates which were unchanged in both experiments ($p > 0.4$). These results, together with the known relationships of β-adrenergic receptor ligand structure to binding affinity and to antagonism/agonism character, lead us to conclude that fluorocarazolol, like carazolol, is in fact a high-affinity β-receptor antagonist.

Biodistribution in Mice. The *in vivo* tissue distributions of (*S*)-(−)-[^{18}F]fluorocarazolol and (*R*)-(+)-[^{18}F]-fluorocarazolol in selected mouse organs after iv injection are presented in Tables 2 and 3. The receptor-blocked experiments were performed after an iv preadministration of 200 μg (6.6 mg/kg) of propranolol. Receptor-specific uptake was calculated as the difference between the total (unblocked experiment) and nonspecific (blocked experiment) binding.

As expected, significant differences ($p < 0.01$) due to receptor blockade with propranolol were observed in the

Table 3. Tissue Distribution of (*R*)-[^{18}F]Fluorocarazolol in Mouse Organs[a]

	time (min)	blood	heart	lung	brain	liver	kidney	bone
nonpro*	10	0.57 ± 0.06	0.93 ± 0.07	8.13 ± 4.06	0.82 ± 0.15	3.08 ± 0.19	4.60 ± 0.47	0.67 ± 0.07
nonpro	20	0.75 ± 0.11	0.81 ± 0.11	5.10 ± 1.81	0.66 ± 0.18	4.00 ± 1.92	4.80 ± 1.40	0.93 ± 0.38
nonpro	40	0.63 ± 0.05	0.76 ± 0.11	3.29 ± 0.97	0.73 ± 0.30	3.00 ± 0.94	3.30 ± 1.17	0.95 ± 0.12
nonpro	60	0.42 ± 0.12	0.56 ± 0.28	2.39 ± 1.10	0.37 ± 0.19	2.56 ± 0.92	2.63 ± 1.13	1.08 ± 0.72
nonpro	90	0.43 ± 0.12	0.46 ± 0.13	1.55 ± 0.77	0.35 ± 0.15	1.25 ± 0.25	1.50 ± 0.63	1.00 ± 0.32
nonpro	120	0.24 ± 0.03	0.28 ± 0.15	1.29 ± 0.19	0.20 ± 0.07	0.94 ± 0.64	1.00 ± 0.13	0.78 ± 0.23
nonpro	180	0.17 ± 0.09	0.14 ± 0.07	0.84 ± 0.19	0.08 ± 0.06	0.78 ± 0.56	0.67 ± 0.30	1.25 ± 0.90
pro**	10	0.92 ± 0.02	1.00 ± 0.06	5.23 ± 0.97	1.04 ± 0.38	3.14 ± 0.19	5.10 ± 0.63	0.67 ± 0.18
pro	20	0.57 ± 0.08	0.85 ± 0.09	3.87 ± 0.39	1.22 ± 0.48	3.00 ± 0.69	4.43 ± 0.70	0.77 ± 0.28
pro	40	0.57 ± 0.08	0.73 ± 0.07	2.00 ± 0.39	0.90 ± 0.22	2.11 ± 0.56	2.70 ± 0.90	0.83 ± 0.08
pro	60	0.63 ± 0.07	0.57 ± 0.06	1.23 ± 0.32	0.62 ± 0.12	1.61 ± 0.42	1.67 ± 0.33	1.15 ± 0.27
pro	90	0.47 ± 0.19	0.48 ± 0.11	1.03 ± 0.45	0.42 ± 0.16	1.17 ± 0.28	1.57 ± 0.70	1.57 ± 1.00
pro	120	0.30 ± 0.17	0.27 ± 0.08	0.45 ± 0.19	0.12 ± 0.06	0.94 ± 0.14	0.63 ± 0.23	1.98 ± 0.87
pro	180	0.09 ± 0.02	0.10 ± 0.05	0.26 ± 0.06	0.06 ± 0.00	0.50 ± 0.42	0.33 ± 0.07	2.98 ± 0.72

[a] Uptake is expressed as (unitless) fractional dose per fractional body weight of the organ. Values are expressed as average ± SD. Data points for heart, brain, blood, lung, kidney, liver, and bone represent five mice at each data point. Data points for other organs represent at least three mice. *: no propranolol preadministration. **: with propranolol preadministration.

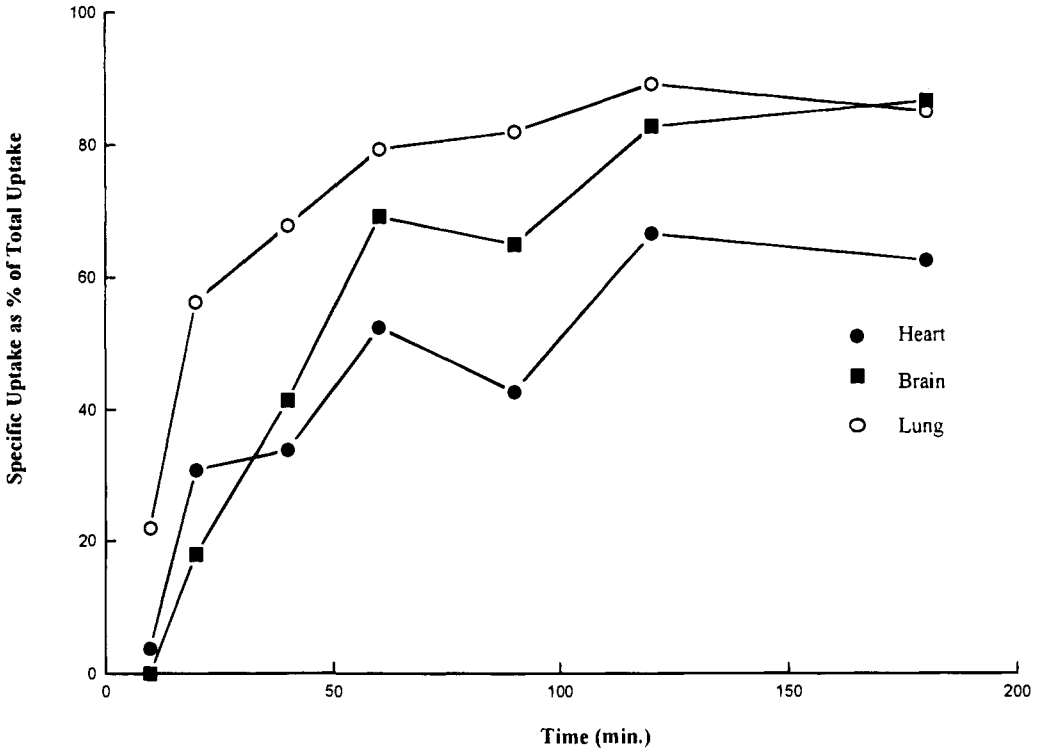

Figure 4. Specific uptake as the percentage of total uptake of (*S*)-[^{18}F]fluorocarazolol in mouse heart, lung, and brain as a function of time. Specific uptake is defined as the difference between the total uptake (untreated) and the nonspecific uptake (propranolol preinjection).

heart, lung, brain, and blood with (*S*)-[^{18}F]fluorocarazolol after 20 min postinjection, indicating specific binding to β-adrenergic receptors. Total binding in most organs (except bone and intestines) decreased over time. However, the maximum specific uptake was achieved at 2 h postinjection in the heart, lung, and blood and at 3 h in the brain. Figure 4 shows the specific uptake as a percentage of the total uptake in heart, lung, and brain at different times. After 2 h postinjection, 86–90% of the total uptake in the brain and lung was specific, while 73–75% of uptake in the heart was specific. The uptake in receptor-poor organs such as kidney, liver, and fat did not change significantly as a result of receptor blockade. In the muscle and spleen, a low receptor-specific uptake was observed after 1 h postinjection. In the small intestine, tracer uptake increased as a result of receptor blockade. This is probably due to nonspecific uptake in this well-perfused organ and/or to hepatobiliary excretion, both of which represent reservoirs for free ligand and could increase as a result of the lack of ligand uptake in other, receptor-rich organs.

The specific uptake of 2-(*R*)-[^{18}F]fluorocarazolol in mouse organs was much lower than that of (*S*)-[^{18}F]-fluorocarazolol because of its significantly lower binding affinity. Table 3 shows that, in all organs except bone regardless of receptor content, no significant difference was observed in uptake of 2-(*R*)-[^{18}F]fluorocarazolol due to receptor blockade by propranolol. This indicates there was no measurable specific binding, as expected. Soon after injection, the (*R*)-[^{18}F]fluorocarazolol uptake in heart, lung, brain, and blood was slightly higher than the nonspecific uptake measured with (*S*)-[^{18}F]fluorocarazolol after propranolol blockade. This may have been due to the relatively low receptor affinity of the ligand. Later, however, the (*R*)-[^{18}F]fluorocarazolol uptake with or without blockade was similar to the measured nonspecific uptake of (*S*)-[^{18}F]fluorocarazolol.

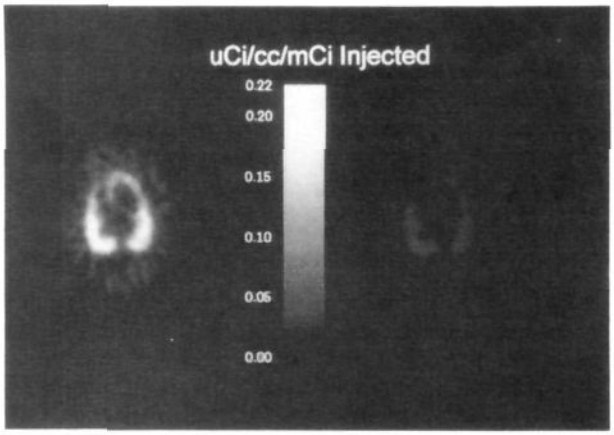

Figure 5. Transaxial PET images of a pig after injection of 1.5 mCi (*S*)-[^{18}F]fluorocarazolol (left image) and after a second (0.9 mCi) radiotracer injection with a preadministration of 3 mg of propranolol iv (right image). Both images represent data gathered between 30 and 60 min pos-injection. Residual activity from the first image was subtracted from the second image. The two images were normalized by dividing the pixel values by the injected dose and were displayed on the same scale.

Bone uptake is caused by release of [^{18}F]fluoride[36,37] during metabolism of the tracer. (*R*)- and (*S*)-[^{18}F]-fluorocarazolol both gave the same bone uptake curve. Initially very low, after 1 h postinjection, the bone radioactivity increased. With propranolol preadministration, bone uptake increased more rapidly for both (*R*)- and (*S*)-fluorocarazolol. The unitless uptake in bone was <3 during the entire measurement period, indicating a reasonably low rate of metabolism of fluorocarazolol in mice.

PET Imaging of Pig Heart and Lung. PET images of a pig using (*S*)-[^{18}F]fluorocarazolol with and without propranolol blockade are shown in Figure 5. Both images represent data gathered between 30 and 60 min after the radiotracer injection. Residual activity from the first injection was subtracted from the second image, and the images were normalized by dividing the pixel values by the injected dose (mCi) and were then displayed on the same scale. In the image of the untreated pig, the heart and lung were clearly seen and easily distinguishable from each other. Administration of propranolol before tracer injection blocked the majority of the uptake of (*S*)-[^{18}F]fluorocarazolol in heart and lung.

The quantified results are shown in Figures 6–8. The figures show the decay-corrected radioactivity content vs time in blood, heart, and lung, respectively. Blood radioactivity (Figure 6) dropped rapidly in the first 3 min to 0.02–0.04 μCi/mL per injected mCi and remained near this range (decay corrected) throughout the study. The blood radioactivity content was not changed by propranolol pretreatment. This allows us to assume that the input functions for the heart and lung were similar with and without propranolol. Uptake in the heart and lung was rapid, and the uptake in the lung was higher than in the heart during the entire time course. The difference between the uptake in the lung and in the heart decreased with time. At 2 min postinjection, the ratio of lung to heart uptake was 2.53, which dropped to 2.0 at 20 min and to 1.4 at 144 min. The washout of the tracer from the tissue after the initial bolus was slow. The heart to blood ratio in the unblocked experiment was 5:7, and the lung to blood ratio was 7:10. A significant decrease in tissue uptake due to propranolol blockade of specific receptor binding was observed as early as 5 min postinjection. Later than 1 h postinjection, more than 77% of the binding in the heart, and 82% in the lung, was displaceable. The specific uptake ratio (specific binding/nonspecific binding) in both organs continued to rise during the study period, reaching a value of 10 by 150 min postinjection. The nonspecific uptake in the lung was higher than in

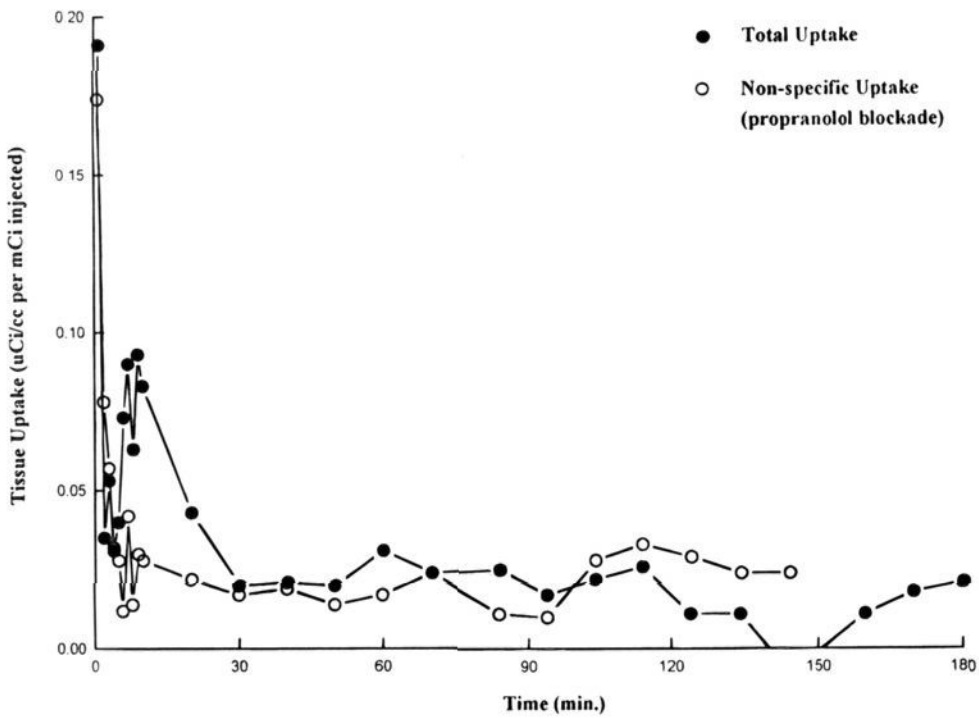

Figure 6. Uptake curve of (*S*)-[^{18}F]fluorocarazolol with and without propranolol blockade in pig blood.

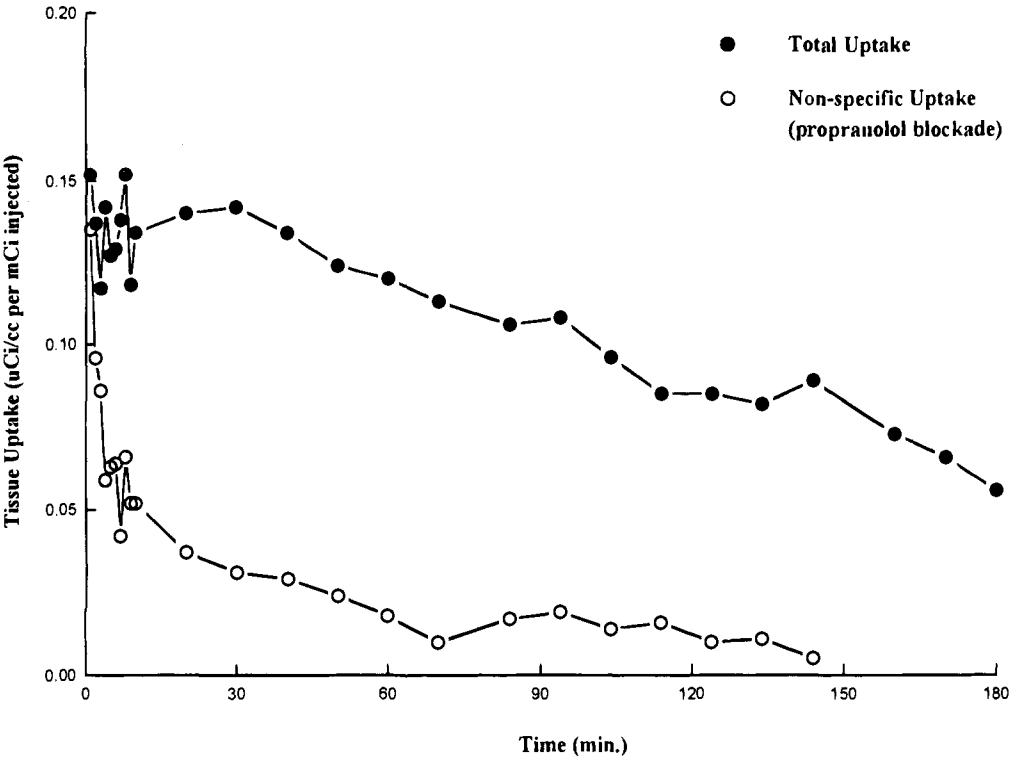

Figure 7. Quantified uptake of (*S*)-[^{18}F]fluorocarazolol with and without propranolol blockade in pig heart. Solid circles represent the uptake of (*S*)-[^{18}F]fluorocarazolol in the untreated animal. Open circles represent the uptake of S-[^{18}F]fluorocarazolol following propranolol administration. Residual activity from the first injection was subtracted from the second injection.

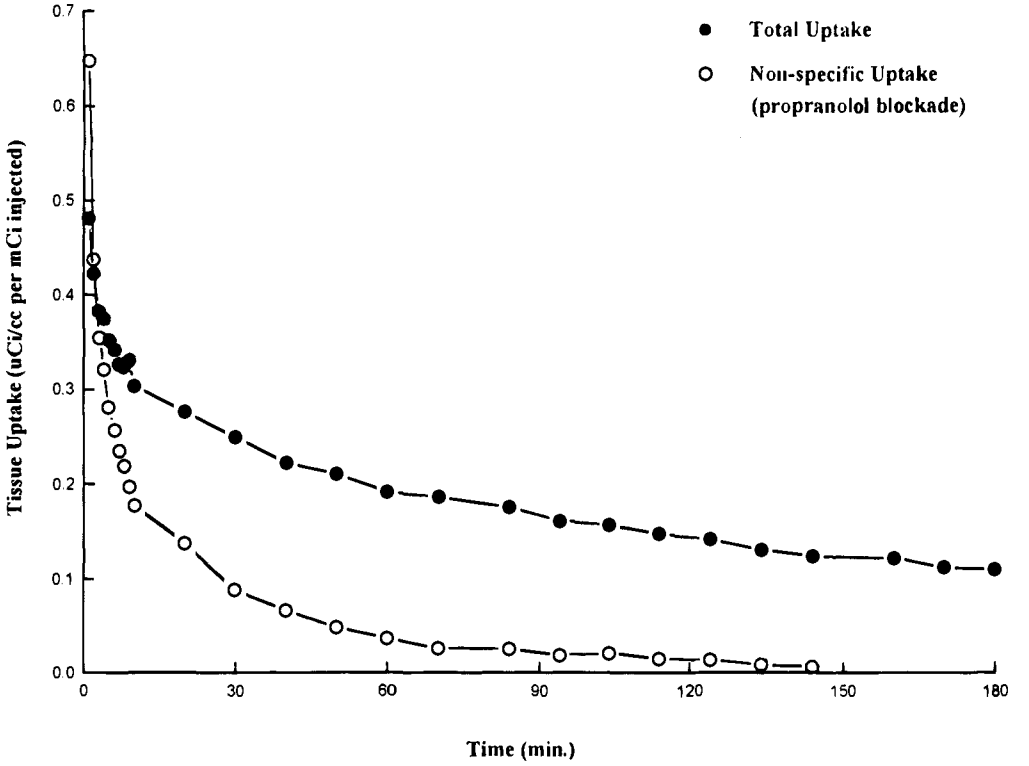

Figure 8. Quantified uptake of (*S*)-[^{18}F]fluorocarazolol with and without propranolol blockade in pig lung. Solid circles represent the uptake of (*S*)-[^{18}F]fluorocarazolol in the untreated animal. Open circles represent the uptake of (*S*)-[^{18}F]fluorocarazolol following propranolol administration. Residual activity from the first injection was subtracted from the second injection.

the heart at early times but equaled that of the heart after 90 min postinjection.

Metabolites of Fluorocarazolol in Blood. Metabolites of fluorocarazolol in the blood were measured between 6 and 120 min postinjection in the pig. Blood samples were centrifuged to separate cells and plasma. The plasma fraction contained fluoride, which was collected on alumina; [^{18}F]fluorocarazolol, which was collected on a reverse-phase cartridge; and labeled polar metabolites, which remained in solution. The radioactivity fractions in the centrifuged pellet and on the reverse-phase cartridge were found, by further extraction with organic solvents and HPLC analysis, to contain >95% [^{18}F]fluorocarazolol. Unmetabolized [^{18}F]-

fluorocarazolol in the plasma represented 72 ± 5% (SD) of the total activity in the blood (ranging from 67% to 82%) and was 78 ± 5% of the radioactivity in plasma. The metabolite fraction was 18% of the total blood activity at 6 min postinjection and increased very slowly over time. Between 15 and 120 min postinjection, the metabolite fraction remained relatively constant at 29 ± 2% of the total blood radioactivity. Fluoride from metabolic defluorination accounted for 15 ± 5% of the total blood activity during the entire time of measurement.

Discussion

The work presented here to prepare and characterize (*S*)- and (*R*)-[^{18}F]fluorocarazolol is an extension of our previous work with [^{11}C]carazolol, a high-affinity β-adrenergic antagonist which showed specific receptor binding observable by PET. The use of an ^{18}F label allowed us to prolong the *in vivo* observation of the radiotracer in tissues of interest to 3 h postinjection. The heart and lung are commonly recognized as containing β-receptors. While there are significant species variations, the β_1-subtype[38,39] is predominant in heart and the β_2-subtype is predominant in lung. The brain also contains β-receptors,[40] and interest in these has been growing in recent years. We feel that labeled carazolol will be a useful radiopharmaceutical for investigation of the β-adrenergic receptors in these tissues. Blood cells have also been shown to have significant β-adrenergic receptor content, probably mainly of the β_2-subtype, in some species[41] including man, and this is a potential complication which may need to be taken into account during future work to apply kinetic models to the quantification of receptors *in vivo*.

Throughout this discussion, we will refer to (*S*)- and (*R*)-fluorocarazolol as counterparts to (*S*)- and (*R*)-carazolol which we previously investigated. Because fluorocarazolol contains a second chiral center which is introduced during the labeling reaction, the terms (*S*)- and (*R*)-fluorocarazolol refer here to a presumably equal mixture of the pair of diastereomers caused by the new chiral center. β-Adrenergic ligands do not generally possess chirality in this position, and the properties of fluorocarazolol and carazolol are very similar. Also, the fluorine atom which is responsible for the asymmetry is not expected to greatly alter the interaction of the ligand with the receptor,on the basis of known structure–activity relationships.[30] We therefore expected that the diastereomers of each pair, if separated, would be indistinguishable by their behavior *in vivo*. In an abstract presented since the completion of this work,[42] it was reported that, as expected, the separated (*S*,*S*)- and (*S*,*R*)-fluorocarazolol diastereomers have identical receptor-binding properties.

As shown in Tables 2 and 3 and Figures 4, 6, and 7, a high level of specific uptake of (*S*)-[^{18}F]fluorocarazolol by β-adrenergic receptors was observed in mice and pigs. In both animals, the total uptake in the lung was much higher than in the heart during the time of measurement. This is expected because the ligand was administered by iv injection, causing all of the injected dose to pass through the lung before reaching the arterial circulation. The lung therefore was able to extract a larger percentage of the injected dose on the first pass than any other organ, resulting in high specific receptor binding as well as high nonspecific uptake at early time points. In the pig experiments, the nonspecific uptake in the lung decreased much faster than in the heart while the specific uptake curve had a similar shape to that of the heart although its magnitude was higher. Slow decreases in the specific uptake curves were observed beginning at 70 min postinjection, which indicated dissociation and washout of the ligand from the receptor. The longer half-life of ^{18}F, as expected, allowed this process to be observed.

The observation of specific uptake of (*S*)-[^{18}F]fluorocarazolol in potential tissues of interest is encouraging and suggests that further work to develop the use of (*S*)-[^{18}F]fluorocarazolol for *in vivo* measurement of β-receptors is justified. Although the specific binding ratio in the mouse heart was relatively low, the ratio observed in heart, lung, and brain would allow receptor-binding measurements to be made if the kinetics are appropriate to existing models. The low specific uptake ratio observed in the mouse heart may be due to the relatively low specific activity of the radiotracer. In fact, with (*S*)-[^{11}C]carazolol, it was shown that an injection of 2 nmol of radiotracer in a mouse was sufficient to completely block the receptors, leaving no evidence of specific binding. An injection of less than 0.25 nmol did allow specific binding to be observed. It is therefore not expected that the dose of fluorocarazolol used here (0.05 nmol or 1.6 nmol/kg) in the mouse would be free of receptor-blocking effects. In the pig, the injected dose was 0.06 nmol/kg and a higher specific uptake ratio was observed. The relatively low specific activity of the tracer was due to the specific activity of the fluoride which we used for labeling and not from the labeling process itself. Other materials have been labeled with this fluoride to give products with similar specific activities. Achievement of higher specific activity is an obviously desirable goal which is separate from this work. Another possibility which we were unable to explore is that the subtype specificity of fluorocarazolol might differ from that of carazolol and be partly responsible for the observed difference in the binding ratio between the two species.

Fluorocarazolol is a lipophilic ligand, and therefore nonspecific uptake was expected to be significant at early times. In the mouse and pig experiments, a dose of propranolol was preadministered to block the receptors and allow measurement of nonspecific tissue uptake of the tracer. This method will not be applicable to human subjects in later studies because a large β-adrenergic blocking dose may lead to cardiac arrhythmia and death. Some receptor kinetic models do not require independent estimation of nonspecific uptake; however it may be necessary or at least advantageous to use an experimental method to estimate the nonspecific tracer uptake. From our results, it appears that (*R*)-[^{18}F]-fluorocarazolol may be useful for this purpose. In mice, it was observed that at 3 h postinjection, the (*R*)-[^{18}F]-fluorocarazolol uptake in untreated animals was similar to the (*S*)-[^{18}F]fluorocarazolol uptake after receptor blockade by propranolol (Figure 9). Although the (*R*)-enantiomer uptake might give a slight overestimation of nonspecific uptake because it does have measurable receptor-binding affinity, no experiments have shown any evidence that significant *in vivo* specific binding is observable with the *R* enantiomer. This is similar to

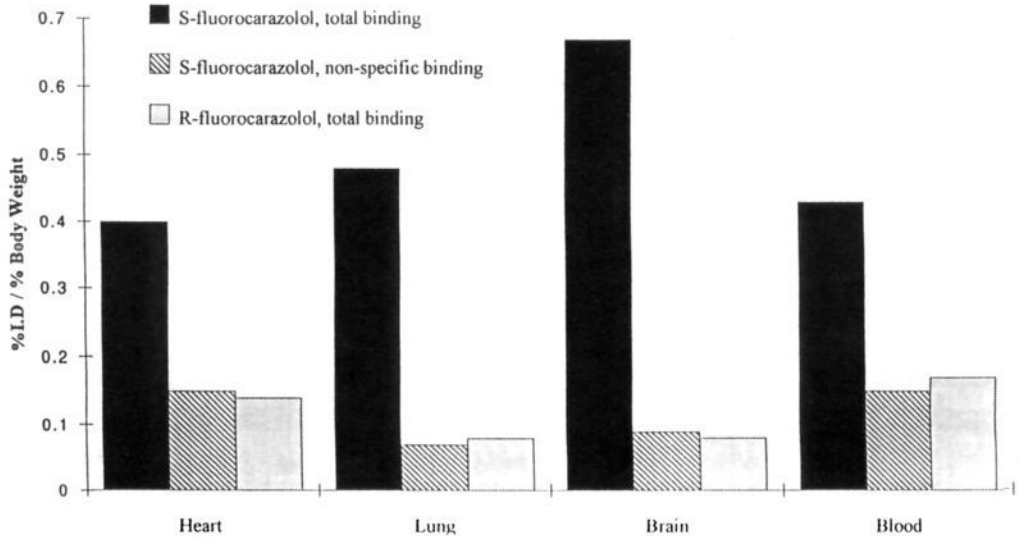

Figure 9. Comparison of (*R*)-[^{18}F]fluorocarazolol total uptake to (*S*)-[^{18}F]fluorocarazolol nonspecific uptake at 3 h postinjection.

previous observations[24-26] with relatively low-affinity carbon-11-labeled β-adrenergic receptor ligands. The advantage of using (*R*)-[^{18}F]fluorocarazolol to measure nonspecific uptake is that the physical properties which are related to nonspecific binding, such as lipophilicity and solubility, must be the same for both enantiomers, but there is no physiological response to the tracer injection, and the specific receptor interaction is not observable by PET.

The ability to correct the blood curve of a receptor-binding radiotracer for the presence of metabolites is important because it affects our ability to apply the kinetic model to the tracer distribution. The concentration of metabolites of fluorocarazolol in the blood remained fairly flat over the entire time of measurement (29 ± 2% between 15 min and 120 min postinjection). Although it is obvious that metabolites must have accumulated in the total body throughout the study, the balance between their production and removal from the blood resulted in a metabolite level in the blood which was almost constant. This simple metabolic profile is similar to that observed for [^{11}C]carazolol and should allow reliable correction of the blood curve for PET studies to be performed with relatively few metabolite analyses.

Experimental Section

Chemical Synthesis. General. Melting points were determined on an Electrothermal capillary apparatus and are uncorrected. Thin layer chromatography was performed on Merck silica gel F-254 glass plates, with visualization by UV (254 nm). Flash column chromatography was performed on Merck silica gel-60 (240 mesh). High-performance liquid chromatography was performed on a Hewlett-Packard 1050 system with a multiwavelength UV detector and monitored at 254, 285, and 315 nm. The column, solvents, and flow parameters are given individually below. Proton NMR spectra were obtained at 200 and/or 300 MHz and are reported in ppm (δ) relative to internal tetramethylsilane (0.00 ppm) or standard solvent peak (CD_3OD, 4.80 ppm; acetone-d_6, 1.96 ppm). Mass spectra were obtained on a Kratos MS25 RFA instrument. Elemental analyses were performed by Galbraith Laboratories, Inc.

Acetol Tosylate (**1**). Method a: To a 500 mL three-necked flask fitted with a stirrer and a thermometer were added 7.41 g (0.1 mmol) of acetol and 30 mL of pyridine. The flask was cooled in an ice–salt bath to below 0 °C. *p*-Toluenesulfonyl chloride (20.74 g, 0.1 mmol) in 70 mL of pyridine was added to the flask over 90–100 min. The temperature was kept below 0 °C during the addition, and the reaction mixture was then stirred at that temperature for 30 min. Iced deionized water (1 L) and 125 mL of 1 N HCl were added, and the mixture was extracted with 2 × 150 mL of methylene chloride. The organic phases were combined and washed with 4 × 200 mL 0.5 N sulfuric acid and 200 mL water and then dried with magnesium sulfate. The methylene chloride was rotary evaporated to afford a light yellow oil. The product was purified by vacuum distillation (0.005 mmHg, bp 70 °C).

Method b: To a 250 mL three-necked flask were added 2 g of hydroxy(tosyloxy)iodobenzene (5 mmol; Aldrich) and 0.36 g (6.2 mmol) of acetone in 100 mL of acetonitrile (freshly distilled from calcium hydride). The mixture was kept under reflux for 2 h before the solvent was rotary evaporated. The residue was dissolved in 50 mL of methylene chloride, washed with 3 × 50 mL of water, dried with magnesium sulfate, passed over a short alumina column, and evaporated. The residue was recrystallized from petroleum ether.

Both methods yielded a white solid. Mp: 34–35 °C (lit.[43] mp 35 °C). TLC: eluent, 3% CH_3OH in CH_2Cl_2; R_f = 0.63. ^{1}H NMR ($CDCl_3$, 200 MHz, TMS added): δ 7.78 (d, aromatic 2H, J = 8 Hz), 7.34 (d, aromatic 2H, J = 8 Hz), 4.45 (s, 2H, CH_2), 2.42 (s, 3H, CH_3), 2.17 (s, 3H, benzyl CH_3). IR: 3062, 2924, 1796, 1600, 1498, 1429, 1368, 1310, 1292, 1190, 1179, 1099, 1038, 972, 860, 789, 766, 668 cm^{-1}.

(*R*)- and (*S*)-Fluorocarazolol ((*R*)-6 and (*S*)-6). (*R*)- or (*S*)-Desisopropylcarazolol[27] ((*R*)-**5**) or (*S*)-**5**; 160 mg, 0.39 mmol) was dissolved in 50 mL of CH_3OH; 50 μL (0.69 mmol) of fluoroacetone (**2**) and 200 μL of acetic acid (3.5 mmol) were added. To this mixture was added dropwise 16.4 mg (0.26 mmol) of sodium cyanoborohydride in 10 mL of CH_3OH. The reaction mixture was then stirred at room temperature for 2 h and the solvent rotary evaporated. The residue was dissolved in 100 mL of CH_2Cl_2, washed with 2 × 100 mL of 0.5 M NaOH and 2 × 100 mL of water, dried with magnesium sulfate, and evaporated. The crude product was chromatographed on silica gel eluted with 2% CH_3OH in CH_2Cl_2 to yield fluorocarazolol ((*R*)-**6** or (*S*)-**6**), 76 mg (62%). TLC: 4% CH_3OH in CH_2Cl_2; R_f = 0.34. HPLC: Alltech econosil silica column, 10 μm, eluted with 1% CH_3OH, 0.02% $MeNH_2$, and 0.02% water in $CHCl_3$, 2 mL/min; t_R = 7.90 min. ^{1}H NMR (CD_3CN): δ 8.26 (d, 1H, J = 8 Hz), 7.47 (d, 1H, J = 8 Hz), 7.36 (t, 1H, J = 7 Hz), 7.31 (t, 1H, J = 8 Hz), 7.18 (t, 1H, J = 7 Hz), 7.10 (d, 1H J = 8 Hz), 6.70 (d, 1H, J = 8 Hz), 4.21–4.37 (m, 2H), 4.06–4.25 (m, 3H), 2.79–3.06 (m, 3H), 1.04 (m, 3H). Optical rotation: 2′-(*S*)(−)-fluorocarazolol diastereomer pair, $[\alpha]_D$ = −13.0° in CH_3OH at room temperature. MS (M^+ calcd for $C_{18}H_{21}N_2O_2F$): 316.2; found, 316.2. HRMS (M^+ calcd for

$C_{18}H_{21}N_2O_2F$): 316.1587; found, 316.1586. Mass spectra were performed for *R* and *S* diastereomer pairs separately.

Fluorocarazolol Hydrochloride. Fluorocarazolol (76 mg; either (*S,S/R*)-**6** or (*R,S/R*-**6**) was dissolved in 10 mL of CH_2Cl_2 and exposed to excess HCl vapor from a 12 N HCl solution in a closed vessel. Fluorocarazolol hydrochloride precipitated as a white solid and was filtered (80 mg, 94%). ^{1}H NMR (CD_3OD): δ 8.15 (d, 1H, J = 7 Hz), 7.32 (d, 1H, J = 8 Hz), 7.23 (t, 1H, J = 7 Hz), 7.21 (t, 1H, J = 8 Hz), 7.05 (d, 1H, J = 8 Hz), 7.02 (d, 1h, J = 7 Hz), 6.61 (d, 1H, J = 8 Hz), 4.34–4.64 (m, 2H), 4.34–4.42 (m, 1H), 4.13–4.29 (m, 2H), 3.58–3.69 (dm, 1H), 3.27–3.48 (m, 2H), 1.17–1.34 (m, 3H). Optical rotations: 2′-(*R*)-(+) diastereomer pair, $[\alpha]_D$ = +18.6° in CH_3OH; 2′-(*S*)-(-) diasteriomer pair, $[\alpha]_D$ = −19.0° in CH_3OH at room temperature. Chiral HPLC: Macherey-Nagel nucleosil chiral 2 column, eluted with 53.5% THF, 46% *n*-heptane, and 0.5% trifluoroacetic acid; t_R (*R*)-fluorocarazolols = 22.2 min, (*S*)-fluorocarazolols = 18.9 and 19.7 min. Elemental analysis was obtained for both diastereomer pairs separately. ($C_{18}H_{22}N_2O_2$-FCl) C, H, N, F.

[^{18}F]Fluoroacetone (2). [^{18}F]Fluoride obtained[44] by 17 MeV proton bombardment of 95+% [^{18}O]water was added to a vessel containing 1.8 mg of potassium carbonate and 13 mg of 4,7,13,16,21,24-hexaoxa-1,10-diazabicyclo[8.8.8]hexacosane (kryptofix 222). The water was evaporated under reduced pressure at 110 °C and recovered. Anhydrous acetonitrile (2 × 2 mL; previously distilled over calcium hydride) was added and evaporated under a helium stream to dry the mixture. A solution of anhydrous acetonitrile (200 μL) containing 2 mg of acetol tosylate (**1**) was added to the reaction vessel which was sealed and heated at 80 °C for 5 min. Then [^{18}F]fluoroacetone (**2**) was distilled along with reaction solvent under a helium stream and collected into 500 μL of dry acetonitrile at 0–5 °C. No other product was detected by HPLC using radiation and refractive index detectors or by GC using a thermoconductivity detector. The product was identified by chromatographic comparison with authentic fluoroacetone (Aldrich Chemical Co.). HPLC: Alltech econosil C-18 column, 10 μm, eluted with water; fluoroacetone t_R = 4.30 min. GC: Alltech RSL 150 capillary column, 55 °C, flow, 4.8 mL of He min^{-1}; fluoroacetone t_R = 3.38 min.

[^{18}F]Fluorocarazolol ((*R*-6) or (*S*)-6). [^{18}F]Fluoroacetone (**2**) was trapped in 500 μL of CH_3OH containing 2.0 mg (6.3 μmol) of (*R*)- or (*S*)-desisopropylcarazolol ((*R*)-**5** or (*S*)-**5**), 4 μL of acetic acid, and 0.1 mg (1.5 μmol) of sodium cyanoborohydride. The reaction mixture was heated to 80 °C for 15 min in a sealed vessel. The solvent was evaporated and the residue dissolved in 500 μL of the HPLC eluent described for unlabeled fluorocarazolol, filtered, and chromatographed. The fraction eluting from 7.8 to 9.5 min was collected. The product identity was verified using the analytical HPLC system described above and by TLC on silica gel eluted with 4% CH_3OH in CH_2Cl_2. R_f's: [^{18}F]fluorocarazolol, 0.34; desisopropylcarazolol, <0.1. The retention times and R_f's were identical for [^{18}F]fluorocarazolol and [^{19}F]fluorocarazolol. No UV-absorbing or radioactive impurities were observed on either system.

***In Vitro* Binding Assay.** Rat hearts were slowly thawed, minced, and homogenized in 20 volumes of ice-cold HEPES-buffered isotonic sucrose (pH brought to 7.4 with Tris base) containing the protease inhibitors (1,10)-phenanthroline (100 μM) and phenylmethanesulfonyl fluoride (50 μM) by using a polytron (Tekmar tissuemizer; at 80 for 2 × 15 s). Homogenates were centrifuged at 1000*g* for 5 min at 4 °C to remove nuclei and debris. The pellets (P1) were resuspended in 20 mL of homogenization buffer and centrifuged again at 1000*g* for 5 min. The combined supernatants were centrifuged at 48000*g* for 18 min at 4 °C, and the resulting P2 pellet was resuspended in 10–25 volumes of 50 mM Tris-HCl buffer (pH 7.7) containing 5 mM EDTA. After recentrifugation at 48000*g* for 18 min, the resulting membrane pellet was resuspended in Tris-HCl containing 25 mM NaCl, preincubated for 30 min at 25 °C, chilled on ice, centrifuged again, resuspended a final time in Tris-HCl alone, centrifuged, flash frozen, and stored at −70 °C. Radioligand-binding assays with [^{125}I]iodopindolol were performed by a modification of methods[45,46] previously described. Membranes were slowly thawed and resuspended in Tris-HCl buffer (50 mM, pH 7.7 at 25 °C) at a concentration of 1 mg of protein/mL. Assays were conducted in a total volume of 250 μL of test compound and (−)-isoproterenol or 0.1% ascorbic acid vehicle. Incubations (60 min at 25 °C) were initiated by the addition of membrane. Nonspecific binding was defined in the presence of (−)-isoproterenol (0.1 mM). Incubations were terminated by vacuum filtration over Reeves-Angel glass fiber filters using a cell harvester (Brandel). The filters were washed four times with 5 mL of ice-cold Tris-HCl and assayed in a gamma counter. Radioligand-binding data were analyzed by nonlinear curve fitting[47] as previously described.

Biodistribution of (*R*)-[^{18}F]6 and (*S*)-[^{18}F]6 in Mice. Male, 25–30 g, CF-1 mice (Charles River Labs) were obtained. Thirty minutes before the tracer injection, the mice were injected with 2 mg of sodium pentobarbital ip and the anesthesia was allowed to take effect. Those mice which were to receive propranolol were then injected via the tail vein with 0.1 mL of 1 mg/mL propranolol iv solution. The labeled (*R*)-[^{18}F]**6** or (*S*)-[^{18}F]**6** was injected through the tail vein approximately 30 min after the propranolol injection. Each mouse received 0.1 mL of solution which contained 1–2 mCi/mL of (*R*)-[^{18}F]**6** or (*S*)-[^{18}F]**6**. At predetermined times after the tracer injection, the mice were sacrificed by cervical dislocation and organs were sampled and placed in weighed vials for counting. Samples were weighed immediately after counting. Each injected dose was weighed by difference in the injection syringe, and the actual injected dose was determined using standards. The standards were prepared by performing two similar weighed injections in 25 mL volumetric flasks and assaying weighed 0.1 mL samples interspersed with the tissue samples. This data was used to calculate uptake in each tissue sample in terms of the percentage of injected dose per gram of tissue (% ID/g). The % ID/g number was then multiplied by the measured body weight of each animal (% ID/g × animal wt/100) to obtain the normalized organ uptake, which is the fractional dose uptake per fractional body weight. The normalized uptake values were unitless and used for group comparisons.

Heart Rate Experiments in Mice. Unanesthetized CF-1 mice (30 g) were injected with propranolol ip (1 mg/mL USP, 0.8 mL, 88 mg/kg) or carazolol or fluorocarazolol iv (5.5 mg/kg, 0.1 mL of 0.5 mg/mL in 20% ethanol in physiological saline USP). At least three observations were made for each condition. In both experiments, control mice received identical injection solutions without drug. The heart rate of each mouse was measured before and 30 min after drug injection.

PET Scanning. Young pigs weighing approximately 30 kg were obtained locally and housed at least 1 day in the university's animal facility. They were anesthetized with sodium pentobarbital and intubated as a precaution against the possibility of respiratory failure. Two 20 G catheters were placed in ear veins for tracer and anesthesia administration during the study. The pigs were kept anesthetized throughout all procedures with incremental administrations of pentobarbital as required. A femoral artery was exposed surgically through which a 6 Fr Cooks pigtail catheter was placed into the descending aorta within 15 cm of the heart and verified by fluoroscopy. A continuous drip of a solution of heparin (10 units/mL) in sterile physiological saline solution was maintained through all catheters, except during injection and blood sampling. Scans were performed on a modified PETT Electronics/Scanditronix Superpett 3000, a time of flight (BaF) scanner with four rings of detectors producing seven tomographic slices. The instrument has an experimentally determined in-plane resolution of 4.8 mm and an axial resolution of 11.5 mm in the low-resolution mode used for this study. Modifications to the scanner included installation of energy discriminators for each detector crystal, an improved time of flight resolution filter, addition of total randoms and continuous dead time corrections, and improved reconstruction software. The reconstruction filters had an in-plane resolution of 12 mm. After each animal was positioned in the scanner with the heart in the center of the scanning zone, a 60 min attenuation measurement was performed using a 3 mCi rotating ^{68}Ge/^{68}Ga source.

The specific activity of (*S*)-[^{18}F]Fluorocarazolol was 300–1200 Ci/mmol and measured at the time of injection. A 2–5 mL bolus injection of 0.9–1.5 mCi of (*S*)-[^{18}F]fluorocarazolol was performed in an ear vein and followed by an immediate 10 mL bolus of normal saline solution to ensure a complete injection. The injection syringe was assayed for radioactivity before and after each injection, and the assays were corrected for decay to the time of injection to calculate the administered dose. List mode data collection was begun at the time of injection and continued for 170 min.

Blood samples were withdrawn at 5 and 10 min intervals throughout the scan both for measurement of blood radioactivity content and for analysis of metabolites. At 170 min after the radiotracer injection, propranolol (3 mg i) was administered. Thirty minutes after the drug administration, a second bolus of (*S*)-[^{18}F]fluorocarazolol was given and the second set of PET scans was begun, following the same procedure as the first. Then a final perfusion scan was performed from 5 to 15 min after injection of 10 mCi of $^{13}NH_3$ for independent delineation of the myocardium.

Data Analysis. The list mode data from the first 10 min of each scan were reconstructed into 10 tomographic images, each representing 1 min of collected data. Additional images were reconstructed from 5 min time intervals beginning 10 min after and continuing to the end of the study. During data reconstruction, the total system count rate, in 1 s time intervals, was used to calculate and apply dead time corrections for each time interval using a paralyzable[48] method, though the count rates from these studies were such that the dead time correction was small. The dead time parameter (τ) was previously determined from phantom studies to be 1.41 s for our system. The images were corrected for random counts using the time of flight (TOF) characteristics of the camera. Random events were assumed to be uniformly distributed across the imaging field prior to the attenuation correction. Events detected in pixels at the periphery of the imaging field at least 16 cm from the subject were measured. The average number of random events per pixel was then adjusted by the attenuation correction factors for each image pixel and subtracted from the image data. This has been validated using phantom studies in which PET data were acquired continuously during decay. In the resulting images, the corrected count total per pixel was converted into units of $\mu Ci/cm^3$ using the camera calibration data.

For each study, the images acquired between 30 and 60 min after injection were summed to produce one high-count, high-contrast image on which regions of interest representing myocardium, lung, and the ventricular cavity were easily defined. The regions of interest were well within, and centered on, their respective areas in order to avoid strong partial volume effects. Other than these precautions, there was no attempt to make corrections for partial volume error. The regions of interest were then applied to the entire sequence of images to generate quantitative time–activity curves for each region during each study. The resultant curves were corrected for the radioactive decay of the label, and the scale was normalized by dividing by the injected dose. In the data from the second set of images, a correction was made for the residual activity in each tissue (heart and lung) which remained from the first injection. The radioactivity which was observed in each region at the end of the first set of data acquisitions (170 min after the first injection) was decay corrected to the beginning of the following scan (210 min after the first injection). That value was taken as the residual activity from the first injection. The decay-corrected value of the residual activity was then subtracted from the decay-corrected curve of the following scan, before normalization for injected dose. Though this technique resulted in a small overcorrection due to the slow decline in the residual activity curve, the error was small relative to the magnitude of the correction.

Metabolism of Fluorocarazolol in Mice and Pigs. Blood samples were taken from mice and pigs at various times after the radioligand injection. For each analysis, 0.5 mL of blood was added to 0.5 mL of ethanol or saline. The samples with ethanol were vortex mixed and ultrasonicated for 5 min. They were then centrifuged in an Eppendorf (Model 5414; 16000*g*) bench-top centrifuge for 6 min, and the supernatant was collected. The pH of the supernatant was then adjusted to about 8 using saturated aqueous potassium bicarbonate. The supernatant was then passed over an neutral alumina cartridge followed by 0.5 mL of ethanol to remove [^{18}F]fluoride. The solution was diluted to 10 mL with water and passed over a Sep-Pak cartridge, which retained unchanged fluorocarazolol. The cartridge was washed with 2 × 10 mL of water to remove metabolites, and then the centrifuged pellet, alumina column, C-18 cartridge, and water fractions were assayed for radioactivity. HPLC confirmed that the radioactivity in the pellet represented more than 95% fluorocarazolol. Independent standards and HPLC were used to verify that the activity in the Sep-Pak cartridge was unchanged fluorocarazolol and the activity in the alumina column was fluoride.

References

(1) Joyce, J. N.; Lexow, N.; Kim, S. J.; Artymyshyn, R.; Senzon, S.; Lawrence, D.; Cassanova, M. F.; Kleinman, J. R.; Bird, E. D.; Winokur, A. Distribution of beta-adrenergic receptor subtypes in human pos-mortem brain: alterations in limbic regions of schizophrenics. *Synapse* **1992**, *10*(3), 228–46.

(2) Kalaria, R. N.; Andorn, A. C.; Tabaton, M.; Whitehouse, P. J.; Karik, S. I.; Unnerstall, J. R. Adrenergic receptors in aging and Alzheimer's disease: Increased β_2-receptors in prefrontal cortex and hippocampus. *J. Neurochem.* **1989**, *53*, 1772–81.

(3) Lemmer, B.; Langer, L., Ohm, T.; Bohl, J. Beta-adrenoceptor density and subtype distribution in cerebellum and hippocampus from patients with Alzheimer's disease. *Naunyn-Schmiedeberg's Arch. Pharmacal.* **1993**, *347*(2), 214–9.

(4) Corwin, J.; Peselow, E.; Feenan, K.; Rotrosen, J.; Fieve, R. Disorders of decision in affective disease: an effect of beta-adrenergic dysfunction? *Biol. Psychiatry* **1990**, *27*, 813–33.

(5) Cole, B. J.; Koob, G. F. Propranolol antagonizes the enhanced conditioned fear produced by corticotropin releasing factor. *J. Pharmacal. Exp. Ther.* **1988**, *247*, 902–10.

(6) Laverdur,e B.; Boulenger, J. P. Beta-blocking drugs and anxiety. A proven therapeutic value. *Encephale* **1991**, *17*, 481–9.

(7) Berridge, C. W.; Dunn, A. J. Restraint-stress-induced changes in exploratory behavior appear to be mediated by norepinephrine-stimulated release of CRF. *J. Neurosci.* **1989**, *9*, 3513–21.

(8) Arango, V.; Ernsberger, P.; Marzuk, P. M.; et al. Autoradiographic demonstration of increased serotonin 5-HT_2 and β-adrenergic receptor binding sites in the brain of suicide victims. *Arch. Gen. Psychiatry* **1990**, *47*, 1038–47.

(9) Otto-Erich, B. β_1 and β_2-Adrenoceptors in the human heart: Properties, function and alterations in chronic heart failure. *Pharm. Rev.* **1988**, *43*, 204–34.

(10) Sibley, D. R.; Lefkowitz, R. J. Molecular mechanisms of receptor desensitization using the β-adrenergic receptor-coupled adenylate cyclase system as a model. *Nature* **1985**, *317*, 124–9.

(11) Lefkowitz, R. J.; Caron, M. G.; Stiles, G. L. Mechanisms of membrane-receptor regulation. Biochemical, physiological and clinical insights derived from studies of the adrenergic receptors. *New Eng. J. Med.* **1984**, *307*, 1570–79.

(12) Barovsky, K.; Brooker, G. (−)-[^{125}I]Iodopindolol, a new highly selective radioiodinated β-adrenergic receptor antagonist: Measurement of β-receptors on intact rat astrocytoma cells. *J. Cyclic Nucleotide Res.* **1980**, *6*, 297–307.

(13) Tondo, L.; Conway, P. G.; Brunswick, D. J. Labeling *In vivo* of beta adrenergic receptors in the central nervous system of the rat after administration of [^{125}I]iodopindolol. *J. Pharmacal. Exp. Ther.* **1985**, *235*, 1–9.

(14) Pazos, A.; Probst, A.; Palacios, J. M. β-Adrenoceptor subtypes in the human brain: autoradiographic localization. *Brain Res.* **1985**, *358*, 324–8.

(15) Ezrailson, E. G.; Garber, A. J.; Munson, P. J.; et al. [^{125}I]-Iodocyanopindolol: A new β-adrenergic receptor probe. *J. Cyclic Nucleotide Res.* **1981**, *7*, 13–26.

(16) Buxton, I. L. O.; Bronton, L. L. Direct analysis of β-adrenergic receptor subtypes on intact adult ventricular myocytes of the rat. *Circ. Res.* **1985**, *56*, 126–132.

(17) Van Dort, M. E.; Gildersleeve, D. L.; Wieland D. M. A rapid high yield synthesis of no carrier added (−)-[^{123}I]-iodocyanopindolol. *Int. J. Radiat. Appl. Instrum.* **1991**, *42*, 309–11.

(18) Mintun, M. A.; Raichle, M. E.; Kilbourn, M. R.; Wooten, G. F.; Welch, M.J. A quantitative model for the *in vivo* assessment of drug binding sites with positron emission tomography. *Ann. Neurol.* **1984**, *15*, 217–227.

(19) Farde, L.; Eriksson, L.; Blomquist, G.; Halldin, C. Kinetic analysis of central [^{11}C]raclopride binding to D_2-dopamine receptors studied by PET- a comparison to the equilibrium analysis. *J. Cereb. Blood Flow Metab.* **1989**, *9*, 696–708.

(20) Arnett, C. D.; Wolf, A. P.; Shiue, C.-Y.; Fowler, J. S.; MacGregor, R. R.; Christman, D. R.; Smith, M. R. Improved delineation of human dopamine receptors using [^{18}F]-*N*-methylspiroperidol and PET. *J. Nucl. Med.* **1986**, *27*, 1878–82.

(21) Perlmutter, J. S.; Larson, K. B.; Raichle, M. E.; Markham, J.; Mintun, M. A.; Kilbourn, M. R.; Welch, M. J. Strategies for *in vivo* measurement of receptor binding using positron emission tomography. *J. Cereb. Blood Flow Metab.* **1986**, *6*, 154–69.
(22) Wong, D. F.; Gjedde, A.; Wagner, H. N. Jr.; Dannals, R. F.; Douglass, K.H.; Links, J. M.; Kuhar, M. J. Quantification of neuroreceptors in the living human brain. II. Inhibition studies of receptor density and affinity. *J. Cereb. Blood Flow Metab.* **1986**, *6*, 147–53.
(23) Huang, S. C.; Barrio, J. R.; Phelps, M. E. Neuroreceptor assay with positron emission tomography: equilibrium versus dynamic approaches. *J. Cereb. Blood Flow Metab.* **1986**, *6*, 515–21.
(24) Berger, G.; Maziere, C.; Prenant, C.; Sastre, J.; Syrota, A.; Comar, D. Synthesis of carbon-11 labeled propranolol. *J. Radioanal. Chem.* **1982**, *74*, 301–4.
(25) Berger, G.; Prenant, C.; Sastre, J.; Syrota, A.; Comar, D. Synthesis of a β-blocker for heart visualization: [^{11}C]-practolol. *Int. J. Appl. Radiat. Isot.* **1983**, *34*, 1556–7.
(26) Prenant, C.; Sastre, J.; Crouzel, C.; Syrota, A. Synthesis of [^{11}C]-pindolol. *J. Labelled Compd. Radiopharm.* **1987**, *24*, 227–32.
(27) Berridge, M. S.; Cassidy, E. H.; Terris, A. H.; Vesselle, J.-M. Preparation and *in vivo* binding of [^{11}C]carazolol, a radiotracer for the beta-adrenergic receptor. *Nucl.Med.Biol.* **1992**, *19*, 563–9.
(28) Delforge, J.; Syrota, A.; Lancon, J.-P.; et al. Cardiac beta-adrenergic receptor density measured in vivo with PET, CGP 12,177, and a new graphical method. *J. Nucl. Med.* **1991**, *32*, 739–48.
(29) Syrota, A. Receptor binding studies of the living heart. *New Concepts Cardiac Imaging* **1988**, *4*, 141–66.
(30) Main, B. G. β-Adrenergic receptors. *Compr. Med. Chem.* **1991**, *3*, 187–228.
(31) Aigbirhio; Pike; Francotte; Waters; Banfield; Jaeggi; Drake. *Tetrahedron: Asymmetry* **1992**; *3*, 539–54.
(32) Elsinga, P. H.; Vos, M. G.; Braker, A. H.; Degroot, T. J.; Van Waarde, A.; Visser, G. M.; Vaalburg, W. Improved synthesis and evaluation of (S,S)- and (S,R)-[^{18}F]-fluorocarazolol, ligands for the visualization of β-adrenergic receptors. *J. Labelled Compd. Radiopharm.* **1994**, *35*, pp 148–9 (abstract).
(33) Buergisser, E.; Hancock, A. A.; Lefkowitz, R. J.; DeLean, A. Anomalous equilibrium binding properties of high affinity racemic radioligands. *Mol. Pharmacol.* **1981**, *19*, 509–12.
(34) Manalan, A. S.; Besch, H. R. Jr.; Watanabe, A. M. Characterization of [^{3}H](±)carazolol binding to β-adrenergic receptors. *Circ. Res.* **1981**, *49*, 326–36.
(35) Stiles, G. L.; Lefkowitz, R. J. Cardiac adrenergic receptors. *Annu. Rev. Med.* **1984**, *35*, 149–65.
(36) Blau, M.; Nagler, W.; Bender, M. A. F-18: A new isotope for bone scanning. *J. Nucl. Med.*, **1962**, *3*, 332–4.
(37) Hein, J. W.; Bonner, J. F.; Brudevold, F.; Smith, F. A.; Hodge, H. C. Distribution in the soft tissue of the rat of radioactive fluoride administered as sodium fluoride. *Nature* **1956**, *178*, 1295–6.
(38) Hedberg, A.; Minneman, K. P.; Molinoff, P. B. Different distribution of beta-1 and beta-2 adrenergic receptors in cat and guinea-pig heart. *J. Pharmacol. Exp. Ther.* **1980**, *212*, 503.
(39) Morris, T. H.; Kaufmann, A. H. Different steric characteristics of β_1- and β_2- adrenoceptors. *Naunyn-Schmiedeberg's Arch. Pharmacol.* **1984**, *327*, 176.
(40) Minneman, K. P.; Wolfe, B. B.; Pittmanl, R. N.; Milinoff, P. B. β-Adrenergic receptor subtypes in rat brain. *Adv. Biochem. Psychopharmacol.* **1983**, *36*, 73–81.
(41) Steer, M. L.; Atlas, D. Demonstration of human platelet β-adrenergic receptors using ^{125}I-cyanopindolol and ^{125}I-hydroxybenzylpindolol. *Biochim. Biophys. Acta* **1982**, *686*, 240–4.
(42) Reference delected in press.
(43) Koser, G. F.; Relenyi, A. G.; Kalos, A. N.; Rebrovic, L.; Wettach, R. H. One-step α-tosyloxylation of ketones with [hydroxy-(tosyloxy)iodo]benzene *J. Org. Chem.* **1982**, *47*, 2487–90.
(44) Tewson, T. J.; Berridge, M. S.; Bolomey, L.; Gould, K. L. Routine production of reactive fluorine-18 fluoride salts from an oxygen-18 water target. *Nucl. Med. Biol.* **1988**, *15*, 499.
(45) Ernsberger, P.; Nelson, D. O. Refeeding hypertension in dietary obesity. *Am. J. Physiol.* **1988**, *254*, R47.
(46) Ernsberger, P.; Iacovitti, L.; Reis, D. J. Astrocytes cultured from specific brain regions differ in their expression of adrenergic binding sites. *Brain Res.* **1990**, *517*, 202.
(47) Motulsky, H. J.; Ransnas, L. A. *RASEB J.* **1987**, *1*, 365.
(48) Sorenson, J. A.; Phelps, M. E. *Physics in Nuclear Medicine*; Grune & Stratton: Philadelphia, 1987; p 254.